Journal of Agriculture and Food Research 17 (2024) 101236

Contents lists available at ScienceDirect

Journal of Agriculture and Food Research

journal homepage: www.sciencedirect.com/journal/journal-of-agriculture-and-food-research

Radiological assessment of both unperturbed and agricultural soils from southern Ecuador

Inmaculada Ramos-Lerate [a,*], Rafael Lozano-Bermejo [b], Juan Ignacio Burneo [c], Chabaco Armijos [d], Manuel Piñero [e], Juan Pedro Bolívar [b], Manuel Jesús Gázquez [a]

[a] Department of Applied Physics, Marine Research Institute (INMAR), University of Cadiz, Campus de Excelencia Internacional del Mar (CEIMAR), Cádiz, Spain
[b] Research Centre of Natural Resources, Health and the Environment (RENSMA), University of Huelva, Campus de Excelencia Internacional del Mar (CEIMAR), Huelva, Spain
[c] Department of Biological and Agricultural Sciences. Universidad Técnica Particular de Loja, San Cayetano Alto s/n, 1101608, Loja, Ecuador
[d] Department of Chemistry. Universidad Técnica Particular de Loja, San Cayetano Alto s/n, 1101608, Loja, Ecuador
[e] Departament of Condensed Matter Physics, University of Cádiz, 11510, Puerto Real, Spain

ARTICLE INFO

Keywords:
Fertilizers
Radiological background
Agricultural soil
Gamma and alpha spectrometry
Radioactive ratio disequilibrium

ABSTRACT

The radiological background in soils across various areas in Southern Ecuador, such as Vilcabamba, Loja, Palanda, Catamayo, and Taquil, was studied to understand the impact of agriculture and fertilizer usage on soil radiological composition. Areas impacted by agricultural activities alongside reference areas unaffected by human intervention were chosen, encompassing comprehensive analyses including gamma and alpha radiation measurements, isotopic ratio determinations, and assessments of radioactive decay chain disequilibrium. Key radiological parameters such as the radium equivalent index, the external gamma absorbed dose rate and the external hazard index were calculated. The external gamma absorbed dose is equal or lower than 57 nGy h^{-1} (mean value worldwide in the Earth's crust). The remaining indexes as well as the annual dose rate are far from the limits allowed for public. Fallout due to ^{137}Cs is negligible and below the minimum detectable activity (MDA). Ratios ^{238}U/^{232}Th varies from 0.55 in Catamayo to 1.11 in Taquil. These values show disequilibrium between the two radioactive chains and it is possible to assume A (^{238}U)~0.64 A (^{232}Th) (excluding Taquil, value 1.11). Furthermore, the radiological composition of commonly used fertilizers, including urea, NPK, NH_4NO_3, KNO_3 and compost, was analyzed, identifying ^{40}K and ^{210}Pb as significant radionuclides. Interestingly, no correlation was found between the types of fertilizers used and the radiological composition of soils. The predominance of the radiological background provided by the parent rock remains the main factor influencing soil composition. The radiological background values for ^{226}Ra, ^{228}Ra, and ^{40}K were established, with a mean value of 23 ± 5 Bq kg^{-1}, 30 ± 4 Bq kg^{-1}, and 450 ± 80 Bq kg^{-1}, respectively. Finally, the distribution of ^{210}Pb in unperturbed soils suggests a higher concentration in the top layer, which is indicative of natural deposition patterns, except in areas affected by erosion such as Vilcabamba, Loja, and Catamayo.

1. Introduction

Radionuclides from ^{238}U, ^{235}U and ^{232}Th series are widely distributed throughout the Earth's crust and some of them, because they are soluble or gaseous, can pass into the hydrosphere and atmosphere during weathering processes [1]. For instance, radium is known by its high solubility and regarding gaseous radionuclides, ^{222}Rn, with a half-life of 3.8 days, may escape from the ground before decay, contrasting with ^{220}Rn, which has a half-life of 54 s and is present in low concentrations in the atmosphere.

Focusing on soils, natural radioactivity is influenced by several factors, including the composition of the bedrock and weathering processes. In undisturbed conditions, radioactive nuclides from natural series within the bedrock (closed systems) are typically in secular equilibrium. However, in open systems like soils, a fraction of ^{222}Rn (a daughter of ^{226}Ra) can exhale into the atmosphere, ranging from 1 % to 30 %, depending on soil properties as granulometry, mineralogy, etc. This ^{222}Rn then decays into ^{210}Pb [2]. Therefore, secular equilibrium is not fulfilled. Once in the atmosphere, ^{210}Pb becomes associated with aerosols and then settles onto the surface [2]. On the other hand, when

* Corresponding author.
E-mail address: inmaculada.ramos@uca.es (I. Ramos-Lerate).

https://doi.org/10.1016/j.jafr.2024.101236
Received 5 April 2024; Received in revised form 18 May 2024; Accepted 30 May 2024
Available online 31 May 2024

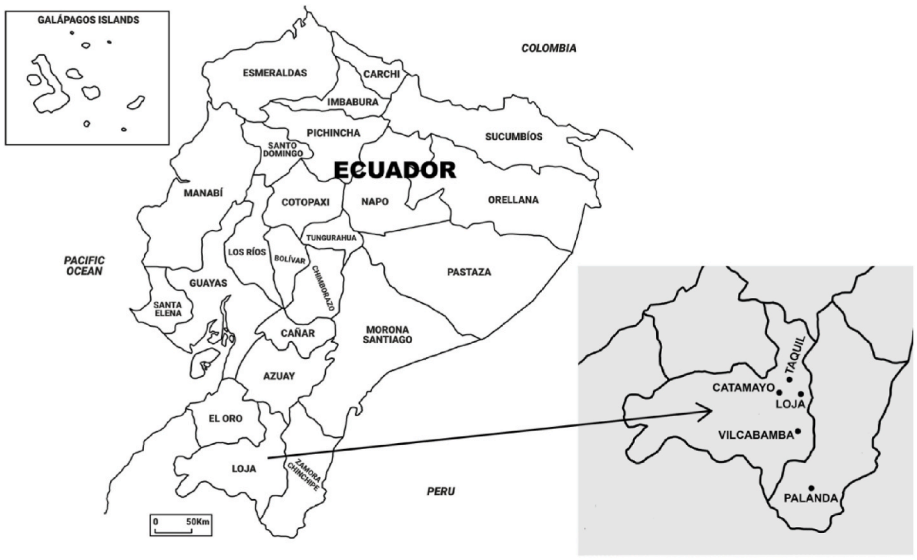

Fig. 1. Location of the samples zones.

bedrock undergoes weathering processes, such as chemical dissolution and physical breakdown, the equilibrium can be disturbed. Weathering can lead to the redistribution of elements and the formation of secondary minerals with different solubilities and precipitation rates. This can result in the preferential retention or release of certain radioactive nuclides, causing disequilibrium within the natural series.

Using gamma and alpha spectrometry, and since the second half of the 20th century, the radioactive backgrounds of the natural series radionuclides have been measured in sediments, hydrosphere and air [3] in a large part of the planet, especially in the northern hemisphere [4–7] and in other areas of the southern hemisphere [8]. Radioisotopes with a half-life greater than the age of the planet have also been measured in nature, such as ^{40}K (gamma emitter) and ^{87}Rb (beta emitter) [9]. Other radioisotopes, such as ^{14}C, ^{3}H, ^{22}Na and ^{7}Be, are also present and continuously formed in the atmosphere as a result of cosmic radiation.

Furthermore, it is also important to mention that some radioisotopes were reintroduced into the environment as a result of nuclear tests that began in the 1960s or as a consequence of nuclear accidents such as Chernobyl in 1986 [10,11] or Fukushima in 2011 [12–14]. The main artificial radionuclides of environmental interest are as follows: ^{137}Cs (gamma emitter with a half-life around 30 years); ^{239}Pu, ^{240}Pu, ^{241}Pu, and ^{241}Am (alpha radionuclides), and ^{90}Sr, ^{3}H, and ^{14}C (beta radionuclides).

The radioactive background of a region reflects the activity of natural radionuclides due to both intrinsic geological factors and the 'fallout' from accidents or nuclear tests. In addition, to assess the radioactive impact, the dose will depend not only on the type of soil and its geology, but also on its altitude at sea level because of the differences in the production of cosmic radiation [15]. Thus, the average of the dose measured at sea level is 0.03 μSv h^{-1}, while at 2000 m it rises to 0.1 μSv h^{-1}. Furthermore, the regional radioactive background can be increased due to Naturally Occurring Radioactive Materials (NORM) industries [16] which handle raw materials and/or by-products and wastes enriched by natural radionuclides. NORM industries includes the extraction of oil and gas, the combustion of fossil fuels, the mining and processing of minerals and the production of phosphate fertilizers, among others.

In the last decade, there has been a growing interest in understanding the environmental implications of intensive fertilizer use on agricultural ecosystems and food products. In this sense, considerable attention has been directed towards assessing the radioactive content of phosphate fertilizers, including NPK complex fertilizers and ammonium phosphates such as di-ammonium phosphate (DAP) and mono-ammonium phosphate (MAP) that are widely used in agricultural soils [17]. Several studies have indicated that production processes of these fertilizers often concentrate radionuclides, particularly isotopes of uranium (^{238}U, ^{235}U and ^{234}U) and ^{230}Th, due to their binding with phosphoric acid—the primary component of these fertilizers [17,18]. Specifically, analyzes have shown that MAP and DAP fertilizers exhibit significantly elevated levels of uranium, with concentrations reaching about 3000 Bq kg^{-1} and 2500 Bq kg^{-1} of ^{238}U, respectively. These concentrations are approximately 100 times higher than those typically observed in undisturbed soils, with an average around 30 Bq kg^{-1} [19]. Similarly, the behavior of ^{230}Th mirrors that of uranium, with activities averaging around 2000 Bq kg^{-1}, approximately 70 times higher than undisturbed soil levels. Conversely, in NPK fertilizers,^{40}K dominates the activity concentrations, that range between 1800 and 4000 Bq kg^{-1}, thus representing a 3-5-fold increase compared with typical soil concentrations, which average around 500 Bq kg^{-1} [19,20].

Extensive radiological studies on soils in the southern region of Ecuador, Loja, have not been published, representing a significant gap in understanding the global radiological background. The absence of this data is relevant not only locally but also globally, as each region contributes to the overall knowledge of environmental radiation. In contrast, numerous studies focused on other parts of the world, mainly on developed regions, such as North America, Europe, some areas of Asia, or Australia, have been published [4–7]. Actually, in Ecuador, prior investigations into natural background radiation have predominantly centered on volcanic regions, particularly within the Chimborazo province, revealing localized increases on radionuclide accumulation in plutonic and metamorphic rocks, as well as volcanic ash dispersed by eruptions from the Sangay volcano [21,22]. However, these investigations were limited to gamma spectrometry measurements of only ^{226}Ra, ^{228}Ra, ^{228}Th and ^{40}K, with no inclusion of alpha measurements or isotopic ratio determinations. Additionally, uranium activities have been assessed in the Napo Formation of the Cretaceous period in Ecuador, renowned for its economically significant phosphate deposits and potential as a hydrocarbon reservoir. The results indicate an average uranium concentration of 100 mg kg^{-1} within the Napo phosphate, accompanied by radioactivity ranging from 20 to 410 Bq kg^{-1} [23]. In contrast, our ongoing study focuses on agricultural zones within Southern Ecuador, diverging from volcanic or commercially-mined areas. In particular, our study focuses on the Loja region (Southern Ecuador), where we have chosen areas impacted by agricultural activities alongside reference areas unaffected by human intervention. Consequently, our research aims to elucidate the radiological impact of

Table 1
Samples: places, number of samples, elevation, coordinates, annual rainfall, average temperature and humidity, principal species cultivated, and type of used fertilizers [26–28].

Place	Samples	Elevation (m a.s.l)	Coordinates	Annual rainfall (mm)/ temperature range/ humidity	Principal species cultivated	Type of fertilized
Vilcabamba	9	1580–1600	4°15′39″ S, 79°13′21″ W	869.7/11–20 °C/78 %	Short-cycle crops, pea beans, coffee, green banana, sweet potato, cassava, guava, avocado, and variety of citrus	No fertilizers
Loja	9	1800–2100	3°53′33.2″ S, 79°15′40.20″ W	956/9–19 °C/71 %	Coffee, green banana, passion fruit, tree tomato, white corn, variety of tubers and vegetables.	No fertilizers
Palanda	9	1120–1210	4°38′59.28″ S, 79°7′55.6″ W	1700/17–20 °C/81 %	Banana, Sugar cane, corn, achiote, coffee, cocoa, cassava, pastures, orange, lemon, tropical and exotic fruits.	Compost
Catamayo	9	700–1010	3°58′48″ S, 79°21′0″ W	350/25–28 °C/53 %	Sugar cane, lemon, cassava, coffee, tomato, bell pepper, cucumber	Urea, NPK purple
Taquil	9	2196–2152	3°54′0"S, 79°18′0″ W	960/12–20 °C/79 %	White corn and barley, livestock pastures	Potassium nitrate, ammonium nitrate

fertilizers (NORM industry) on these soils, encompassing comprehensive analyses including gamma and alpha radiation measurements, isotopic ratio determinations, and assessments of radioactive decay chain disequilibrium. For this purpose, the activity concentrations of various natural radionuclides (^{238}U, ^{235}U, ^{234}U, ^{232}Th, ^{230}Th, ^{228}Th, ^{210}Po, ^{210}Pb, ^{226}Ra, ^{228}Ra, and ^{40}K) present in soils have been measured, as well as the artificial radionuclide ^{137}Cs. In general, the deposition of ^{137}Cs in the soil is usually limited to the first 10 cm [20,24], since it is rapidly absorbed specially on organic matter and clays [25]. Significantly, to ensure the accuracy of background radiation values, our study incorporates robust statistical analyses. This rigorous statistical framework enhances the reliability and significance of the natural background for all the region. The existence of radiological background data in regions not studied to date, such as soils in Southern Ecuador, contributes to understanding the effects of radiation and its distribution on the planet. Actually, the determination of the radiological background is crucial to study present or future impacts associated with NORM industries or to control possible damage to ecosystems produced by future nuclear accidents.

Building upon the radiological background discussed earlier, the goal of this study is to analyze the radiological impact of agricultural practices, both with and without fertilizer usage, on soils in the Loja region. Particularly noteworthy is the phosphate fertilizer industry, a NORM sector that has the potential to increase exposure to ionizing radiation by concentrating natural radionuclides. This increase can be transmitted to crops and pass through the food chain. Despite this intensive use, it is important to assess whether doses are lower than the permitted dose limits to avoid damage to both the environment and the population itself. Therefore, agricultural soils with different types of fertilizers or treatments have been analyzed by examining both radionuclide concentrations at surface levels and various depths up to 40 cm to assess mobility and leaching patterns.

2. Materials and methods

2.1. Site characteristics and sampling

This study focuses on the Loja region, which is in Southern Ecuador (Fig. 1). Sampling zones were carefully selected to assess the potential impact of agricultural practices on soil radioactivity levels. Furthermore, these zones represent various geological soil types prevalent in the region.

Notably, the Vilcabamba and Loja sites were identified as the regions where conventional fertilizers are not used in agricultural practices. In contrast, compost is used in Palanda, urea and NPK (nitrogen, phosphorus, and potassium) fertilizers in Catamayo, and KNO3 (potassium nitrate) in Taquil.

The different types of fertilizers used by farmers in these areas were also analyzed to fully understand the impact of agriculture on soil contamination. This analysis aimed to quantify the degree of soil contamination related to fertilizer use, thus providing valuable insights into the agricultural contribution to overall soil radioactivity levels.

In the five sites chosen for the study (Vilcabamba, Loja, Palanda, Catamayo, and Taquil), samples were taken in the form of columns up to 40 cm deep, subdividing each column into three different depths for analysis (the depth of the first zone was from 0 to 5 cm, the second zone from 5 to 20 cm, and the third zone from 20 to 40 cm). Moreover, samples of the soils undisturbed by agriculture or anthropogenic activities (i.e., control soils) were compared with samples of agricultural soils. The samples codes are as follows: control soil (C), agricultural soil with no fertilizers (NF), and agricultural soil with fertilizers (YF).

Likewise, C samples were used to determine the radiological background and fallout of the area, and NF samples were used to study the radiological impact of agricultural activity without fertilizers, compared with C samples. On the other hand, YF samples were used to assess the impact associated with the use of fertilizers. Furthermore, the analysis of columns has made it possible to verify the degree of affectation by leaching.

Table 1 shows the locations of the sample points (latitude, longitude and elevation), the number of samples and the type of fertilizers used in each location. The annual rainfall (mm), the temperature range (°C), the humidity (%) and the principal cultivated species are also included in this Table for each location [26–28]. After collecting the columns and separating them by depth, the samples were dried and milled below 100 μm particle size previously to the alpha and gamma analysis.

2.2. XRF analysis

The major elements were determined by X-ray fluorescence (XRF) using a Bruker S4 Pioneer system (4 kW, Rh front window and anode, five analyzing crystals [LIF200, Ge, PET, OVO55, and OVOC], and two X-ray detectors). One gram of sample was ground and mixed with both 10 g of lithium tetraborate and 5 drops of 20 % lithium iodide to obtain a homogenous glass for examination.

2.3. Gamma spectrometry

The samples were measured by gamma spectrometry using a thin-window well HPGe detector with a full-width at half-maximum (FWHM) of 1.33 keV at 122 keV (^{57}Co) and 2.04 keV at 1332 keV (^{60}Co), and a peak/Compton ratio of 56.2/1. The detector was coupled to a multichannel analyzer and shielded with a thickness layer of 10 cm Pb plus 2 mm of Cu to avoid interferences from X-ray from the lead. The full energy peak efficiency calibration was conducted using the solid RGU-1 Standard Reference Material, obtained from the International Atomic Energy Agency (IAEA), with a known amount of ^{238}U (4940 ±

30 Bq kg^{-1}) and with all its daughter products in secular equilibrium. Absorption corrections were made for the measurements following previously established methods [29]. The following radionuclides were measured using these gamma peaks: ^{210}Pb at 46.5 keV (intensity 4.05 %), ^{234}Th (^{238}U) at 63.29 keV (intensity 3.84 %), ^{214}Pb (^{226}Ra) at 351.92 keV (intensity 35.1 %), ^{228}Ac (^{228}Ra) at 911.07 keV (intensity 27.07 %), and ^{40}K at 1460.83 keV (intensity 10.67 %).

2.4. Alpha spectrometry

In all samples, U-isotopes (^{234}U, ^{235}U, and ^{238}U), Th-isotopes (^{232}Th, and ^{230}Th), and ^{210}Po activity concentrations were determined by alpha-particle spectrometry after applying a sequential radiochemical procedure.

A 1 g aliquot of each selected sample was dissolved using microwave acid digestion (hydrochloric, hydrofluoric, nitric, and perchloric acids), followed by passage through a UTEVA (Uranium and TetraValents Actinides) chromatographic resin (provided by Eichrom Technologies Inc., Lisle, IL, USA) as 2 % nitric acid solutions. This process aimed to isolate U, Th, and Po according to the methodology explained in detail in Ref. [30].

The U- and Th-isotopes are electrodeposited onto stainless steel planchets, following the method of Hallstadius [31], while the polonium (after conditioning the Po fraction) is self-deposited onto silver discs [32,33]. The recovery yields obtained by this radiochemical procedure ranged between 80 and 90 % for both U and Po, while for Th they were in the order between 50 % and 60 % [30,34,35].

The alpha-particle determinations were carried out through the use of an EG&G Ortec alpha-particle spectrometer system comprising eight chambers, each one equipped with a 450 mm^2 ion-implanted semiconductor detector (PIPS type), which provides an efficiency of around 25 % for our counting geometry.

2.5. Statistical analysis

The Grubbs' test is a statistical method designed to identify outliers within a Gaussian dataset. It operates by comparing the deviation of a suspected outlier from the dataset's mean with a critical threshold. The G-observed, or experimental value of this statistic variable, is calculated as the maximum absolute difference between individual values and the mean of the dataset, divided by the standard deviation of the dataset, while the G-critical value depends on the sample size (n) and the significance level (α) chosen (in our case, $\alpha = 0.05$). The G-critical value, denoted as G-critical, represents the threshold beyond which a data point is considered an outlier. It serves as a reference point for determining the significance of the calculated G-value. Statistical methods were utilized to evaluate the normality of the dataset, representing preliminary procedures preceding the application of the Grubbs' test. Normality assessments, including the Shapiro-Wilk, Anderson-Darling, and Lilliefors tests, were conducted to ascertain the distribution of the data and verify its statistical robustness. The statistical software used was XLSTAT (https://www.xlstat.com/en/), developed by Lumivero.

Additionally, the z-score (a statistical measure indicating how many standard deviations a value is from the mean of a dataset) was included. When the z-score falls within the range of −2 to 2, it indicates that these values are within two standard deviations of the mean. As the Grubbs test compares the most extreme value (the farthest from the mean) with the expected distribution, if the absolute z-score is greater than the G-critical, then the data point is considered an outlier.

2.6. External effective doses

Radium equivalent index, external absorbed gamma dose rate and external hazard index were calculated in all samples. Radium equivalent index is the radium equivalent radioactivity to represent the specific activity of ^{226}Ra, ^{232}Th and ^{40}K (radium activity giving the same gamma dose as the combined activity of the three series ^{238}U, ^{232}Th and ^{40}K in secular equilibrium). This concept allows to describe the radiation hazard from the three different radionuclides mixture with a single index. It was calculated assuming that 370 Bq kg^{-1} of ^{226}Ra, 259 Bq kg^{-1} of ^{232}Th and 4810 Bq kg^{-1} of ^{40}K produce the same gamma-ray dose rate and according to equation (1) [36–39].

$$Ra_{eq} = A_{Ra} + 1.43\ A_{th} + 0.077\ A_K \quad \text{[eq. 1]}$$

where all activities concentrations are expressed in Bq kg^{-1}.

On the other hand, the external absorbed gamma dose rate (D_{abs}) in nGy h^{-1} was assessed. This dose describes the gamma dose absorbed by the public exposed to ^{226}Ra, ^{228}Ra and ^{40}K in outdoor air at 1 m height above the ground and was estimated using equation (2) [40,41].

$$D_{abs} = 0.462C_{Ra\text{-}226} + 0.662C_{Ra\text{-}228} + 0.043C_{K\text{-}40} \quad \text{[eq. 2]}$$

Where $C_{Ra\text{-}226}$, $C_{Ra\text{-}228}$ and $C_{K\text{-}40}$ are the activity concentrations of ^{226}Ra, ^{228}Ra and ^{40}K, respectively, in Bq kg^{-1}.

Mean Typical values about 57 nGy h^{-1} are typical for soils in unperturbed areas [19,41]. The permissible limit of D_{abs} must be less than 0.059 mGy h^{-1} or 59,000 nGy h^{-1} [19,38].

The effective annual dose rate is the conversion factor from the external absorbed gamma dose rate in the air to the effective dose 0.7 Sv Gy^{-1} (upper limit if we consider outdoor occupancy factor like 1).

Finally, the external hazard index, I_{ex}, was also assessed. This index was firstly defined by Beretka and Mathew [39] with the goal to limit the radiation dose to a dose equivalent limit of 1 mSv y^{-1} which is the maximum dose allowed for general public [19]. The external hazard index (I_{ex}) was calculated using equation (3) [42]:

$$I_{ex} = A_{Ra}/370 + A_{Th}/259 + A_K/4810 \quad \text{[eq. 3]}$$

I_{ex} should not exceed the limit of 1 for the radiation hazard to be negligible.

Table 2
XRF results of the soils unperturbed by agriculture at the different locations (average values).

Element	Vilcabamba %	Loja %	Palanda %	Catamayo %	Taquil %
Al	7.67	7.86	6.54	9.29	9.55
Ba	0.07	0.07	0.09	0.06	0.07
Ca	0.54	0.02	2.69	1.51	1.10
Fe	3.04	3.26	4.07	4.65	4.26
K	3.15	2.51	2.90	2.05	2.69
Mg	0.78	0.75	1.24	1.13	0.90
Mn	0.08	0.09	0.10	0.07	0.10
Na	0.47	0.51	0.75	0.66	0.75
P	0.15	0.11	0.19	0.08	0.08
S	0.08	0.08	0.11	0.06	0.04
Si	30.6	29.7	22.6	27.4	28.3
Ti	0.41	0.37	0.50	0.54	0.44

Table 3
Results from DRX with Rietveld refinement converged. N.D. (Not Detected).

Name	Vilcabamba	Loja	Palanda	Catamayo	Taquil
Silicon oxide	60	50	46	47	59
Muscovite	11	37	14	11	16
Chlorite	10	<1.0	N.D	5.1	N.D
Biotite	6.3	1.3	14	6.0	2.8
Anorthite	6.1	5.7	7.3	12	7.4
Kaolinite	3.8	2.0	N.D	7.3	N.D
Albite	2.0	1.9	5.3	8.7	3.3
Vermiculite	<1.0	<1.0	N.D	2.7	12

Table 4
Gamma Activity Concentrations (Bq kg^{-1}) in each Location.

	Sample	^{210}Pb	^{234}Th (^{238}U)	^{214}Pb (^{226}Ra)	^{228}Ac (^{228}Ra)	^{40}K
VILCABAMBA	V1C-0-5	42 ± 6	25 ± 5	25.6 ± 1.5	33 ± 4	520 ± 30
	V1C-5-20	31 ± 5	28 ± 4	21.8 ± 1.4	29 ± 3	510 ± 30
	V1C-20-35	24 ± 4	26 ± 4	22.9 ± 1.2	32 ± 3	480 ± 23
	V2NF-0-5	22 ± 5	22 ± 4	13.9 ± 1.1	25 ± 3	357 ± 21
	V2NF-5-20	13 ± 5	18 ± 4	16.0 ± 1.2	25 ± 3	342 ± 21
	V2NF-20-35	11 ± 4	16 ± 4	17.5 ± 1.1	22 ± 3	383 ± 21
	V3NF-0-5	16 ± 5	21 ± 4	19.2 ± 1.3	28 ± 3	394 ± 23
	V3NF-5-20	19 ± 4	24 ± 4	18.0 ± 1.1	24 ± 3	382 ± 21
	V3NF-20-35	13 ± 4	22 ± 4	15.1 ± 1.0	25 ± 3	378 ± 18
LOJA	L1C-0-5	39 ± 6	27 ± 5	21.5 ± 1.4	29 ± 3	414 ± 24
	L1C-5-20	27 ± 5	23 ± 4	20.3 ± 1.3	28 ± 3	427 ± 24
	L1C-20-35	22 ± 4	22 ± 4	20.5 ± 1.2	28 ± 3	430 ± 24
	L2NF-0-5	15 ± 5	21 ± 4	18.6 ± 1.4	26 ± 4	400 ± 30
	L2NF-5-20	23 ± 5	21 ± 4	24.1 ± 1.5	34 ± 3	500 ± 30
	L2NF-20-35	19 ± 4	23 ± 4	21.8 ± 1.3	36 ± 3	560 ± 30
PALANDA	P1C-0-5	106 ± 8	26 ± 5	25.3 ± 1.8	28 ± 4	470 ± 30
	P1C-5-20	25 ± 5	11 ± 7	23.7 ± 1.5	33 ± 4	640 ± 30
	P1C-20-35	16 ± 4	29 ± 4	22.4 ± 1.2	30 ± 3	570 ± 30
	P2YF-0-5	56 ± 6	29 ± 5	20.4 ± 1.5	29 ± 4	490 ± 30
	P2YF-5-20	42 ± 6	26 ± 5	24.5 ± 1.5	37 ± 4	500 ± 30
	P2YF-20-35	22 ± 5	39 ± 5	27.7 ± 1.6	38 ± 4	490 ± 30
	P3YF-0-5	52 ± 6	26 ± 5	18.3 ± 1.4	23 ± 4	490 ± 30
	P3YF-5-20	16 ± 5	33 ± 5	22.9 ± 1.5	28 ± 3	520 ± 30
	P3YF-20-35	17 ± 5	30 ± 5	28.1 ± 1.6	31 ± 3	620 ± 30
CATAMAYO	C1C-0-5	13 ± 5	28 ± 4	18.3 ± 1.2	25 ± 3	339 ± 21
	C1C-5-20	20 ± 5	19 ± 4	21.0 ± 1.4	31 ± 3	396 ± 23
	C1C-20-35	22 ± 5	30 ± 5	24.2 ± 1.5	27 ± 3	412 ± 24
	C2NF-0-5	23 ± 5	32 ± 4	21.1 ± 1.3	34 ± 3	382 ± 22
	C2NF-5-20	14 ± 4	23 ± 4	20.2 ± 1.2	24 ± 3	362 ± 20
	C2NF-20-35	15 ± 4	18 ± 4	18.2 ± 1.2	26 ± 3	301 ± 19
	C3YF-0-5	14 ± 4	21 ± 4	21.8 ± 1.2	31 ± 3	365 ± 19
	C3YF-5-20	18 ± 5	24 ± 4	20.9 ± 1.3	30 ± 3	399 ± 22
	C3YF-20-35	20 ± 5	27 ± 4	20.8 ± 1.3	21 ± 3	348 ± 20
TAQUIL	T1C-0-5	96 ± 5	27 ± 4	31.4 ± 1.7	31 ± 3	520 ± 30
	T1C-5-20	30 ± 5	35 ± 5	29.0 ± 1.6	33 ± 3	470 ± 30
	T1C-20-35	22 ± 4	32 ± 5	30.7 ± 1.6	27 ± 3	470 ± 24
	T2YF-0-5	22 ± 5	32 ± 5	30.9 ± 1.7	32 ± 3	490 ± 30
	T2YF-5-20	20 ± 5	28 ± 5	25.7 ± 1.4	36 ± 3	426 ± 23
	T2YF-20-35	27 ± 5	28 ± 5	32.3 ± 1.7	37 ± 3	480 ± 30
	T3NF-0-5	25 ± 5	34 ± 5	29.0 ± 1.7	33 ± 4	440 ± 30
	T3NF-5-20	24 ± 5	30 ± 5	26.9 ± 1.6	38 ± 4	410 ± 30
	T3NF-20-35	31 ± 5	30 ± 5	30.0 ± 1.7	32 ± 3	420 ± 30

3. Results and discussion

3.1. Chemical and mineralogical characterization

For this study, soils non perturbed by agriculture collected in wild areas of similar characteristics to the ones used in agricultural activities were analyzed by XRF and DRX. A priori, the chosen sampling zones represent diverse geological soil types prevalent in the region, although the results in Table 2 and Table 3 show a similar geochemical background.

Mean values in Table 2 have been calculated for each location with three samples and the associated error is less than 10 %. The results showed that the chemical composition of soils were quite similar, with Al, Fe, K and Si being the main elements. Percentages between 0.5 and 1 % were found for Mg, Na, and Ti.

The mineralogical phases are included in Table 3, which show a major presence of quartz (between 45 and 60 %) and muscovite (between 11 and 37 %) in most areas. Except in Palanda, which presented a larger presence of biotite (14 %) than the remaining places, the percentages of other phases in all locations were lower than 10 %, with average differences of about 5 %. In supplementary materials, Fig. S1, a representative DRX graphic is presented for each location. There were no significant differences in relation to depth.

To sum up, although the sampling zones represented several soil types prevalent in the region, the geochemical analysis revealed a striking similarity in the geochemical background across all sampled areas. As the soils at the different sampling locations had similar composition and mineralogy, differences in natural radioactivity should not be very significant, driving to a similar radiometric fingerprint.

3.2. Natural radionuclides activity concentrations

Table 4 shows the gamma results for radionuclides of interest at the different locations. However, ^{137}Cs was not reported as it was always below the Minimum Detectable Activity (MDA; 2 Bq kg^{-1}). This result is consistent with the fact that most nuclear tests and accidents have taken place in northern hemisphere.

For the control samples (unperturbed by agricultural activities), ^{210}Pb activity shows a maximum value in the top 5 cm of soil in Palanda and Taquil (106 and 96 Bq kg^{-1}, respectively), decreasing to a mean value of 25 Bq kg^{-1} at depths of (20–35) cm in these two locations. This is the expected result for the concentration of ^{210}Pb in an unperturbed area [43,44] where concentrations are higher in the first centimeters of the sediment column. However, for the remaining locations (control samples or not), the values of ^{210}Pb are similar in all areas and depths with a minimum in the 20–25 cm layer in Vilcabamba (about 11 Bq kg^{-1}). Besides, it cannot be asseverated that there is a general activity gradient according to the depth of the sample as the highest values of activities for ^{210}Pb can be found in any layer (at the top, bottom or intermediate layer). As in Vilcabamba, Loja and Catamayo the concentration of ^{210}Pb was not greater in the first centimeters of the control

Table 5
Mean Activity Concentration ± Standard Deviation (Bq kg^{-1}).

		^{210}Pb	^{234}Th (^{238}U)	^{214}Pb (^{226}Ra)	^{228}Ac (^{228}Ra)	^{40}K
VILCABAMBA	CONTROL	32 ± 9	26.4 ± 1.7	23.4 ± 1.9	31.2 ± 2.0	501 ± 19
	NO FERT.	16 ± 4	20 ± 3	16.6 ± 2.0	24.9 ± 2.0	373 ± 19
LOJA	CONTROL	29 ± 9	24 ± 3	21.0 ± 0.6	28.0 ± 0.7	425 ± 10
	NO FERT.	19 ± 4	21.6 ± 1.3	21 ± 3	32 ± 6	490 ± 80
PALANDA	CONTROL	50 ± 50	22 ± 10	23.7 ± 1.5	30 ± 3	560 ± 80
	FERT.	34 ± 18	31 ± 5	24 ± 4	31 ± 6	520 ± 50
CATAMAYO	CONTROL	18 ± 5	26 ± 6	21 ± 3	28 ± 3	380 ± 40
	NO FERT.	17 ± 5	24 ± 7	19.9 ± 1.5	28 ± 5	350 ± 40
	FERT.	16 ± 3	24.6 ± 2.4	22.1 ± 1.2	29 ± 4	380 ± 30
TAQUIL	CONTROL	49 ± 41	31 ± 4	30.3 ± 1.2	30 ± 3	480 ± 30
	NO FERT.	23 ± 4	30 ± 3	30 ± 3	35 ± 3	470 ± 40
	FERT.	27 ± 4	31.4 ± 2.2	28.7 ± 1.6	34 ± 3	426 ± 15

sample (unperturbed soil), this result could only be explained if the soils have been altered (e.g., through erosion phenomena).

^{234}Th (^{238}U) ranges from a minimum of 11 Bq kg^{-1} to a maximum of 39 Bq kg^{-1}, both in Palanda. Additionally, no general gradient of activities depending on the depth of the sample can be found (Table 4). Mean values (Table 5) are very similar for all locations and depths, ranging between 20 and 31 Bq kg^{-1} and therefore no significant influence of the agricultural activities can be shown through the activity of this radionuclide. As for the control samples, the mean value is the same in all locations within uncertainties, so there is no gamma radiometric fingerprint due to ^{234}Th (^{238}U) in agreement with the characterization of the soils (quite similar in elements and mineral phases). For this radionuclide, a general gamma radiometric fingerprint of around (25 ± 7) Bq kg^{-1} was concluded for all control soils.

^{214}Pb (^{226}Ra) ranges from 13.9 Bq kg^{-1} in Vilcabamba to 32.3 Bq kg^{-1} in Taquil. As previously with the radionuclides from the ^{238}U radioactive chain, Table 4 shows that there is no gradient of activities. Considering all samples (unperturbed soils and agricultural soils), mean values (Table 5) are very similar for all locations and depths, ranging between 16.6 and 30.3 Bq kg^{-1}. Therefore, no significant influence of agriculture can be shown through this radionuclide. Regarding control soils, mean values are also quite similar, being slightly higher in Taquil (30.3 ± 1.2 Bq kg^{-1}) compared to the rest of the locations (21 ± 3 Bq kg^{-1}). Since the composition and mineralogy is quite similar in all locations, this slightly different radiometric fingerprint in Taquil is probably related to a different ratio U/Th, as alpha analysis will show in following paragraphs.

The results of Tables 4 and 5 show that, except for the higher values of ^{210}Pb, there is a secular equilibrium in all the gamma radionuclides in the ^{238}U radioactive chain.

On the other hand, ^{228}Ac (^{228}Ra), from the ^{232}Th radioactive chain, shows an activity concentration range from 21 Bq kg^{-1} in Catamayo to 38 Bq kg^{-1} in Taquil. Additionally, there is no gradient of activities, as can be seen in Table 4, and the mean values (in Table 5) are very similar for all locations and depths, ranging between 24.9 and 35 Bq kg^{-1}. Once again, a common gamma radiometric fingerprint can be associated with all locations, as mean values within uncertainties are the same in all control samples, around (30 ± 3) Bq kg^{-1}.

The ^{40}K activity concentrations in soil are very similar in all the studied areas (Table 4). The maximum activity was found in Loja with 640 Bq kg^{-1}, and the minimum in Catamayo with 301 Bq kg^{-1}. There is no gradient of activities depending on depth and the mean values (Table 5) are very similar for all locations and depths, ranging between 373 and 560 Bq kg^{-1}. As for control samples, ^{40}K activities result in a slightly different radiometric fingerprint. In fact, it can be established that the range of (500 ± 80) Bq kg^{-1}covers the values obtained in Vilcabamba, Palanda and Taquil and (400 ± 50) Bq kg^{-1} covers those obtained in Loja and Catamayo.

Table 6
Activity concentrations (Bq kg^{-1}) in fertilizers.

	Type of fertilizer	^{40}K	^{210}Pb	^{234}Th (^{238}U)	^{214}Pb (^{226}Ra)	^{228}Ac (^{228}Ra)
PALANDA	COMPOST	685 ± 40	64 ± 5	23.0 ± 2.1	20 ± 2	20 ± 2
CATAMAYO	UREA	300 ± 20	<28	<15	<10	<15
	NPK	7080 ± 123	<23	<12	<7	15.0 ± 2.1
TAQUIL	KNO_3	10,580 ± 250	<22	9.0 ± 1.1	<10	5.0 ± 1.4

Fertilizers samples were also measured by gamma spectrometry. It is important to remember that fertilizers were not used in Loja and Vilcabamba, whereas compost was used in Palanda, urea and NPK in Catamayo, and KNO_3 in Taquil. Table 6 shows the activity concentrations for the various fertilizers. The only significant radionuclides in all fertilizers were ^{40}K, covering from 300 Bq kg^{-1} in urea to 10,580 Bq kg^{-1} in KNO_3, and^{210}Pb in compost. The remaining radionuclides were lower than the MDA or the control sample activity in soils, except in Palanda where the ^{238}U activity of the compost was similar to the activity of the control soil (where no fertilizer was used).

Comparing the values for ^{40}K activity in Tables 4 and in Tables 6 and it is interesting to highlight the maximum ^{40}K activity in Loja, 640 Bq kg^{-1}, where no fertilizers are added to the soil, while the minimum is in Catamayo, where urea and NPK (7080 Bq kg^{-1} of ^{40}K, as seen in Table 3) were added to the soil. This difference may be attributed to the severe soil erosion reported in Catamayo sites [45], which results in soil deterioration and depletion of nutrients [46], likely due to extensive agriculture over many years. Consequently, the addition of fertilizers is necessary for crop growth. According to the measurements, the ^{40}K concentrations from fertilizers could be incorporated by crops. In Taquil, KNO_3 is used as a fertilizer, with a^{40}K activity concentration of 10,580 Bq kg^{-1} (Table 6). However, Table 5 shows that the mean activity concentration of ^{40}K in Taquil is about 430 Bq kg^{-1} in fertilized soil, 480 Bq kg^{-1} in control soil and 470 Bq kg^{-1} in soil without fertilizer.

On the other hand, Table 6 shows a value of 64 Bq kg^{-1} for ^{210}Pb in compost. This value could be compatible with those in Table 4 for Palanda, where compost is also used. Actually, samples with fertilizers in Palanda show that the ^{210}Pb activity concentration was 56 and 52 Bq kg^{-1} in the first layer.

For ^{210}Pb, the activity in the control sample is higher than in soils perturbed by agriculture, and this reduction of activity concentrations in cultivated areas may be attributed to the assimilation of soil components by the plants. For the remaining radionuclides, except in Vilcabamba, it is observed from Table 5 that activity concentrations are quite similar in control samples (unperturbed soil) and soils perturbed by agricultural activities (with or without fertilizer). However, in Vilcabamba, soils perturbed by agricultural activities show lower activities than control soils, indicating that the radionuclides are incorporated into the food chain.

Alpha spectrometry analysis was used to verify secular equilibrium in both natural series. For this purpose, four locations were chosen: Vilcabamba, Palanda, Catamayo and Taquil. Vilcabamba and Loja did not use fertilizers, so Vilcabamba was selected as representative of soil without fertilizer. One control sample and one sample of cultivated soil without fertilizer were chosen in Vilcabamba; samples of the control soil

Table 7
Alpha Activity Concentration (Bq kg^{-1}) in each location.

	Sample	^{210}Po	^{230}Th	^{232}Th	^{234}U	^{238}U
VILCABAMBA	V1C-0-5	42.8 ± 2.3	–	–	20.6 ± 1.4	21.7 ± 1.5
	V3NF-0-5	20.7 ± 1.6	18.8 ± 1.6	29.5 ± 1.8	19.0 ± 1.5	18.3 ± 1.5
PALANDA	P1C-0-5	123 ± 5	–	–	16.6 ± 1.4	19.7 ± 1.5
	P3YF-0-5	51 ± 3	16 ± 3	27 ± 3	18.8 ± 1.7	20.3 ± 1.7
CATAMAYO	C1C-0-5	25.3 ± 1.5	19.1 ± 1.4	32.1 ± 1.8	18.7 ± 1.4	17.6 ± 1.4
	C2NF-0-5	20.5 ± 1.4	23.2 ± 2.1	32.4 ± 2.4	16.6 ± 1.7	19.4 ± 1.9
	C3YF-0-5	22.3 ± 1.1	25 ± 3	32 ± 3	18.0 ± 1.5	22.7 ± 1.9
TAQUIL	T1C-0-5	92 ± 3	30 ± 5	30 ± 5	34.7 ± 2.3	33 ± 3

and soil with fertilizer (compost) were measured in Palanda, and one sample of control soil, one sample of cultivated soil without fertilizers, and one sample of cultivated soil with fertilizers (NPK and urea) were measured in Catamayo. Finally, only control soil was measured with an alpha spectrometer in Taquil. All samples were collected from the 0–5 cm depth.

From Table 7, ^{210}Po activity concentrations vary from 20.5 Bq kg^{-1} in Catamayo to 123 Bq kg^{-1} in Palanda. When comparing this data with the ^{210}Pb data from Tables 4 and it can be deduced that there is secular equilibrium between ^{210}Pb and its daughter ^{210}Po. For example, in Palanda's control area, the ^{210}Pb activity concentration in the first layer is 106 Bq kg^{-1} and the ^{210}Po activity concentration is 123 Bq kg^{-1}; in Taquil's control area, the ^{210}Pb activity concentration in the first layer is 96 Bq kg^{-1} and ^{210}Po activity concentration is 92 Bq kg^{-1}. This conclusion is further supported by data from Table 8, where it can be observed that the ratios of ^{210}Pb/^{210}Po are very close to unity (with two exceptions in Catamayo, where the ratio of ^{210}Pb/^{210}Po is close to 0.5).

Likewise, ^{230}Th activity concentrations vary from 16 Bq kg^{-1} in Palanda to 30 Bq kg^{-1} in Taquil. Similar values can be found for ^{234}U and ^{238}U, varying from 16.6 Bq kg^{-1} in Palanda and Catamayo to 34.7 Bq kg^{-1} in Taquil, and from 17.6 Bq kg^{-1} in Catamayo to 33 Bq kg^{-1} in Taquil, respectively. It can be affirmed that all the radioelements in the ^{238}U radioactive chain are in secular equilibrium. It can be observed too in Table 8, where ^{234}U/^{238}U ratios are very near to the unity, varying from 0.79 to 1.06, both in Catamayo. And also, from Table 8, the ratios of ^{238}U/^{226}Ra are very close to the unity varying from 0.78 to 1.11, both in Palanda.

In addition, ^{232}Th activity concentrations vary from 27 Bq kg^{-1} in Palanda to 32.4 Bq kg^{-1} in Catamayo. All the samples present a similar activity, close to 30 Bq kg^{-1}. Tables 4 and 5 show the activity of ^{228}Ac (^{228}Ra), which was also around 30 Bq kg^{-1}. This secular equilibrium between ^{232}Th and its daughters ^{228}Ac (^{228}Ra) was therefore confirmed.

The ^{238}U/^{232}Th ratios vary from 0.55 in Catamayo to 1.11 in Taquil. These values show disequilibrium between the two radioactive chains. Table 7 shows that the radionuclides belonging to the ^{238}U chain were about 20 Bq kg^{-1}, whereas the radionuclides belonging to the ^{232}Th chain were about 30 Bq kg^{-1}. This was also seen in control samples, both fertilizer and no fertilizer samples, so it may be concluded that there is disequilibrium between the ^{238}U radioactive chain and the ^{232}Th radioactive chain in the studied areas in Ecuador. Considering the ^{238}U/^{232}Th ratios from Tables 8 and it was assumed that in this area A (^{238}U) ~ 0.64 · A (^{232}Th) in soils of the areas studied (excluding the value of 1.11 in Taquil). If we compare with the gamma radiometric fingerprint, this fact agrees that Taquil is the only place where we have found a slightly different gamma radiometric fingerprint compared to other locations (for ^{214}Pb (^{226}Ra) we have found concentrations in Taquil about (30.3 ± 1.2) Bq kg^{-1} compared to (21 ± 3) Bq kg^{-1} in the rest of the locations).

The radiological background in soils in our locations in Ecuador has been compared with activities in soils around the world, as shown in Table 9. The mean activity concentration of ^{238}U worldwide is 36 Bq kg^{-1} [19]. Values vary from 8.4 in Srirangam (India) [47] to 79 Bq kg^{-1} in Lombardia [48], Italy. Data obtained in Ecuador are about 25 Bq kg^{-1}, quite similar to the ^{238}U mean activity worldwide.

The mean activity concentration of ^{226}Ra is 35 Bq kg^{-1} worldwide [19], due to the secular equilibrium in the ^{238}U radioactive chain. Values range from 18 Bq kg^{-1} in Um Hablayn (Saudi Arabia) [49] to 88 Bq kg^{-1} in Espírito Santo (Brazil) [50], with values about 50 Bq kg^{-1} in both

Table 8
Activity ratios in each location.

	Sample	^{234}U/^{238}U	^{238}U/^{232}Th	^{238}U/^{226}Ra	^{210}Pb/^{210}Po
VILCABAMBA	V1C-0-5	0.95 ± 0.09	–	0.85 ± 0.08	0.98 ± 0.15
	V3NF-0-5	1.04 ± 0.12	0.62 ± 0.07	0.95 ± 0.10	0.8 ± 0.3
PALANDA	P1C-0-5	0.84 ± 0.10	–	0.78 ± 0.08	0.87 ± 0.07
	P3YF-0-5	0.93 ± 0.12	0.74 ± 0.12	1.11 ± 0.13	1.02 ± 0.13
CATAMAYO	C1C-0-5	1.06 ± 0.12	0.55 ± 0.05	0.96 ± 0.10	0.51 ± 0.20
	C2NF-0-5	0.85 ± 0.12	0.60 ± 0.07	0.92 ± 0.10	1.1 ± 0.3
	C3YF-0-5	0.79 ± 0.10	0.71 ± 0.09	0.99 ± 0.11	0.67 ± 0.23
TAQUIL	T1C-0-5	1.04 ± 0.12	1.11 ± 0.21	1.06 ± 0.12	1.04 ± 0.07

Table 9
Mean Activity Concentrations (Bq kg^{-1}) and mean ratios in soils in several places in the World.

PlaceI	^{238}U	^{226}Ra	^{232}Th	^{40}K	^{238}U/^{232}Th	^{238}U/^{226}Ra	Reference
Worldwide average	**36**	**35**	**30**	**400**	**1.2**	**1.03**	UNSCEAR [19]
Um Hablayn, Saudi Arabia	–	18.11	16.12	1603.73	1.37	1.58	[49]
Srirangam, India	8.4	–	98.4	436	0.09	–	[47]
Ercek Lake, Turkey	18.9	–	27.2	524	0.69	–	[52]
Lombardia, Italy	79	–	48	640	1.65	–	[48]
Salamanca, Mexico	10–42	11–50	11–51	178–811	–	0.7–1.2	[41]
Espírito Santo State, Brasil	–	11–88	18–424	7–693	–	–	[50]
South-western Nigeria	–	52.91	76.79	393.73	–	–	[51]
Vilcabamba, Ecuador	23 ± 5	21 ± 3	30 ± 4	500 ± 80	0.62 ± 0.07	0.90 ± 0.10	Present Study
Palanda, Ecuador	23 ± 5	21 ± 3	30 ± 4	500 ± 80	0.74 ± 0.12	0.95 ± 0.10	
Catamayo, Ecuador	23 ± 5	21 ± 3	30 ± 4	400 ± 50	0.62 ± 0.07	0.96 ± 0.10	
Taquil, Ecuador	23 ± 5	30 ± 2	30 ± 4	500 ± 80	1.11 ± 0.21	1.06 ± 0.12	

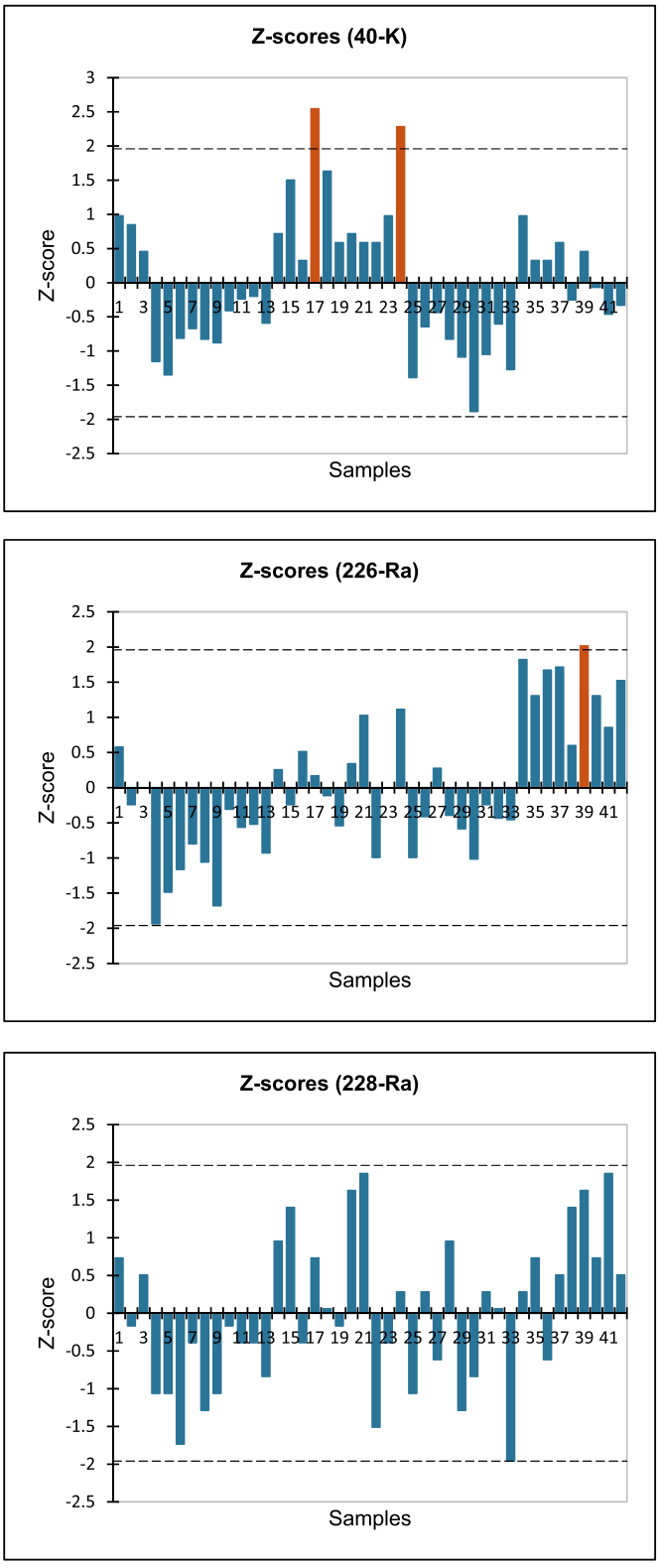

Fig. 2. Z-scores for three different radionuclide activities measured at 42 locations in this study. The Z-score is a statistical measure indicating how many standard deviations a value is deviated from the dataset average.

Salamanca (Mexico) [41] and South-western Nigeria [51]. For comparison, in Vilcabamba, Palanda and Catamayo, the ^{226}Ra activity concentrations are around 21 Bq kg^{-1}, whereas in Taquil is around 30 Bq kg^{-1}. The general secular equilibrium in the ^{238}U radioactive chain and

Table 10
Mean values (± standard deviation) of external absorbed gamma dose, radium equivalent and external hazard index.

		D_{abs} (nGy h^{-1})	Rae (Bq kg^{-1})	Iex
VILCABAMBA	CONTROL	52 ± 2	107 ± 3	0.288 ± 0.008
	NO FERT.	40 ± 1	81 ± 2	0.219 ± 0.005
LOJA	CONTROL	45 ± 1	94 ± 1	0.254 ± 0.002
	NO FERT.	51 ± 5	105 ± 9	0.283 ± 0.025
PALANDA	CONTROL	54 ± 3	110 ± 5	0.297 ± 0.015
	FERT.	52 ± 1	108 ± 2	0.291 ± 0.006
CATAMAYO	CONTROL	44 ± 2	90 ± 5	0.244 ± 0.013
	NO FERT.	43 ± 3	86 ± 6	0.233 ± 0.018
	FERT.	45 ± 2	93 ± 3	0.250 ± 0.008
TAQUIL	CONTROL	54 ± 1	109 ± 4	0.250 ± 0.009
	NO FERT.	56 ± 2	114 ± 3	0.311 ± 0.009
	FERT.	53 ± 1	113 ± 2	0.306 ± 0.005
Mean Value		53 ± 4	101 ± 15	0.269 ± 0.009

in particular, the secular equilibrium between ^{238}U and ^{226}Ra is confirmed by the ^{238}U/^{226}Ra ratios: the worldwide data is 1.03 [19]. This ratio is 1.58 in Um Hablayn (Saudita Arabia) [49], whereas in the four places in Ecuador is about the unity, range from 0.90 in Vilcamba to 1.06 in Taquil.

For ^{232}Th activity concentrations, the worldwide value is 30 Bq kg^{-1}. The values for different places range from 27.2 Bq kg^{-1} in Turkey [52] to 98.4 Bq kg^{-1} in Srirangam (India) [47], and exceed 400 Bq kg^{-1} in some places in Brazil [50]. The values obtained in the localions in Ecuador are all around 30 Bq kg^{-1}, consistent with the worldwide value.

The ^{238}U/^{232}Th ratios varies from 0.09 in Srirangam (India) to 1.65 in Lombardia, Italy. The worldwide mean for this ratio is 1.2. The values found in Ecuador fall within this range, and are very similar to the value found in Ercek Lake (Turkey), with the exception of the value in Taquil. It is concluded that there is a big amplitude of values, and in all cases the ^{238}U/^{232}Th ratio is lower than 2.

Moreover, ^{40}K is of special interest in soils due to fertilizers used in agriculture. The mean activity concentration worldwide for this radionuclide is 400 Bq kg^{-1}. In agriculture soils ^{40}K ranges from 400 Bq kg^{-1} in Catamayo (Ecuador) to 1603 Bq kg^{-1} in Um Hablayn (Saudita Arabia), being the majority of values between 400 and 600 Bq kg^{-1}. Therefore, extra ^{40}K, introduced by the adding of fertilizers to soils, are absorbed by plants, as these data show.

Finally, the distribution of ^{210}Pb in unperturbed soils suggests a higher concentration at the top layer, which is an indicative of natural deposition patterns, except in Vilcabamba, Loja, and Catamayo, where alterations in soils are apparent (erosion areas).

We can conclude there is no correlation between the types of fertilizers used and the radiological composition of soils: the predominance of the radiological background provided by the parent rock from which soils originate remains the primary factor influencing soil composition in the studied areas. This allows for a more in-depth statistical analysis of all the data to verify if the radiological background we have determined is significant.

The normality of the dataset for ^{226}Ra, ^{228}Ra and ^{40}K comprising all samples in this study was assessed using three different tests: Shapiro-Wilk, Anderson-Darling, and Lilliefors. Results provided robust evidence supporting that all datasets exhibited normal distributions ($p > 0.05$). This allow to employ Grubbs' test to identify potential outliers within the dataset.

In the case of ^{226}Ra, only one sample is above the G-observed value (2.014) but it is still below the critical value (G-critical value is 3.057). The same happens with ^{40}K in two samples (G-observed value is 2.545, G-critical value 3.057) corresponding to Palanda (P3YF-20-35 and P1C-5–20). In the case of ^{228}Ra, no significant outliers were found (see Fig. 2).

We can conclude the results show homogeneity within the dataset, suggesting robustness and consistency in the measured values. This

allows to assess a radiological background for the whole region being 23 ± 5 (13.9–32.3) Bq kg^{-1} the mean value for ^{226}Ra, 30 ± 4 (21–38) Bq kg^{-1} for ^{228}Ra and 450 ± 80 (300–640) Bq kg^{-1} the mean value for ^{40}K.

3.3. Doses

As explained in Section 2.6, radium equivalent index (Rae), external absorbed gamma dose rate (Dabs), and external hazard index (Iex) were calculated in all samples. The mean values are shown in Table 10. Detailed results for all locations and depths can be found in supplementary materials (Table S1), as well as $^{226}Ra/^{228}Ra$ and $^{40}K/^{226}Ra$.

From Table 10, we can conclude that the use of fertilizers does not influence the external dose received by the population as there is no increase over the background levels (control areas). This finding is consistent regardless of the type of fertilizer used (compost in Palanda, urea and NPK in Catamayo and KNO_3 in Taquil).

On the other hand, the radium equivalent index and the external absorbed gamma dose rate, are similar or lower than the worldwide mean values (57 nGy h^{-1} for the external absorbed gamma dose rate, and 100 Bq kg^{-1} for the radium equivalent index [19]). The external hazard index if far below 1, so radiation hazard was negligible. Furthermore, the homogeneity within the dataset for all samples (non-perturbed and agricultural soils) regarding the radium equivalent index, the external gamma dose rate and the hazard index was established through normality tests (Shapiro-Wilk, Anderson-Darling, and Lilliefors). The results showed normal distributions ($p > 0.05$) and no outlier within the dataset. Table 10 also includes the results of the mean values.

4. Conclusions

In this study the impact associated with fertilizer use in agricultural activities was analyzed in Southern Ecuador, as the fertilizer industry falls under Naturally Occurring Radioactive Materials (NORM) industries.

Characterization of the soils show that the composition and mineralogy are quite similar in all locations. On the other hand, the ratio of $^{238}U/^{232}Th$ varies from 1.1 in Taquil to 0.55 in Catamayo, showing a clear disequilibrium between both natural radionuclide series. For ^{40}K, the radiometric fingerprint can be established as (500 ± 80) Bq kg^{-1} for Vilcabamba, Palanda and Taquil and (400 ± 50) Bq $kg^{-1}$for Loja and Catamayo. Additionally, this study found that in soils dedicated to agriculture, there was no observed increase in radiation dose above natural background levels, regardless of the type of fertilizer utilized. Furthermore, the homogeneity within the dataset allows mean values to be established in all the region, thus determining a radiological background for the whole area. Southern Ecuador radiological background values are: (23 ± 5) Bq kg^{-1} for ^{226}Ra activity, (30 ± 4) Bq kg^{-1} for ^{228}Ra activity, (450 ± 80) Bq kg^{-1} for ^{40}K, (53 ± 4) nGy h^{-1} for external gamma dose, (101 ± 15) Bq kg^{-1} for Radium equivalent. Finally, fertilizers samples have also been measured radiologically. The only significant radionuclide is ^{40}K with values ranging from 300 Bq kg^{-1} to 685 Bq kg^{-1} in urea and compost to 7080 Bq kg^{-1} and 10,580 Bq kg^{-1} in NPK and KNO_3.

Finally, ^{210}Pb results in soils unperturbed by agriculture indicate a maximum of activity within the first 5 cm in Palanda and Taquil, about 100 Bq kg^{-1}, decreasing to a mean value of 25 Bq kg^{-1} at depths of (5–35) cm. This result is consistent with unperturbed areas where $^{210}Pb/^{210}Po$ concentrations are expected to be higher in the top layers. However, this is not observed in Vilcabamba, Loja and Catamay, which can be attributed to erosion phenomena affecting these sampling sites.

CRediT authorship contribution statement

Inmaculada Ramos-Lerate: Writing – original draft, Formal analysis, Conceptualization. **Rafael Lozano-Bermejo:** Data curation. **Juan Ignacio Burneo:** Data curation. **Chabaco Armijos:** Data curation. **Manuel Piñero:** Data curation. **Juan Pedro Bolívar:** Writing – review & editing, Supervision, Funding acquisition. **Manuel Jesús Gázquez:** Writing – review & editing, Supervision, Methodology, Funding acquisition, Data curation.

Declaration of competing interest

The authors declare that they have no known competing financial interests or personal relationships that could have appeared to influence the work reported in this paper.

Data availability

Data will be made available on request.

Acknowledgements

This research was funded by the following projects: Operative FEDER Program-Andalucía 2014–2020 (UHU-1255876, UHU-202020); GrantsPID2020-116461RB-C21 and 116461RA-C22 funded by MICIU/AEI/10.13039/501100011033; Grant TED2021-130361B–I00 funded by MICIU/AEI/10.13039/501100011033 and, by "European Union Next Generation EU/PRTR", and Campus de Excelencia Internacional del Mar (CEIMAR) (research project CEIJ-C07.2)

Appendix A. Supplementary data

Supplementary data to this article can be found online at https://doi.org/10.1016/j.jafr.2024.101236.

References

[1] M. García-León, Detecting Environmental Radioactivity, Springer International Publishing AG, 2022.
[2] P. Gmbh, B. Allee, Application of 210-pb in soils, J. Paleolimnol. 13 (1989) (1995) 157–168.
[3] R.L. Lozano, J.P. Bolívar, E.G. San Miguel, R. García-Tenorio, M.J. Gázquez, An accurate method to measure alpha-emitting natural radionuclides in atmospheric filters: application in two NORM industries, Nucl. Instruments Methods Phys. Res. Sect. A Accel. Spectrometers, Detect. Assoc. Equip. 659 (1) (Dec. 2011) 557–568, https://doi.org/10.1016/J.NIMA.2011.08.006.
[4] I. Ramos-Lerate, M. Barrera, R.A. Ligero, M. Casas-Ruiz, Radionuclides in the environment of the bay of cadiz, Radiat. Protect. Dosim. 75 (1998) 41–48, https://doi.org/10.1093/oxfordjournals.rpd.a032244. International Symposium on Radionuclides in the Oceans-Distributions, Models and Impacts (RADOC 96-97) PU-NUCLEAR TECHNOLOGY PUBL PI-ASHFORD PA-PO BOX 7, ASHFORD, KENT, ENGLAND TN23 1YW.
[5] A. Abbasi, F. Mirekhtiary, Heavy metals and natural radioactivity concentration in sediments of the Mediterranean Sea coast, Mar. Pollut. Bull. 154 (2020), https://doi.org/10.1016/j.marpolbul.2020.111041.
[6] V. Strati, et al., Total natural radioactivity, Veneto (Italy), J. Maps 11 (4) (2015), https://doi.org/10.1080/17445647.2014.923348.
[7] B.A. Al-Mur, A. Gad, Radiation hazard from natural radioactivity in the marine sediment of jeddah coast, red sea, Saudi Arabia, J. Mar. Sci. Eng. 10 (8) (2022), https://doi.org/10.3390/jmse10081145.
[8] R. da Costa Dantas, J.A. Navoni, F.L.S. de Alencar, L.A. da Costa Xavier, V.S. do Amaral, Natural radioactivity in Brazil: a systematic review, Environ. Sci. Pollut. Control Ser. 27 (1) (2020), https://doi.org/10.1007/s11356-019-06962-6.
[9] A.G. Carles, K. Kossert, Measurement of the shape-factor functions of the long-lived radionuclides 87Rb, 40K and 10Be, Nucl. Instruments Methods Phys. Res. Sect. A Accel. Spectrometers, Detect. Assoc. Equip. 572 (2) (2007), https://doi.org/10.1016/j.nima.2006.11.064.
[10] V.A. Kashparov, et al., Territory contamination with the radionuclides representing the fuel component of Chernobyl fallout, Sci. Total Environ. 317 (1–3) (2003), https://doi.org/10.1016/S0048-9697(03)00336-X.
[11] M. Jönsson, et al., Modelling the external radiation exposure from the Chernobyl fallout using data from the Swedish municipality measurement system, J. Environ. Radioact. (2017) 178–179, https://doi.org/10.1016/j.jenvrad.2017.07.003.
[12] G. Steinhauser, A. Brandl, T.E. Johnson, Comparison of the Chernobyl and Fukushima nuclear accidents: a review of the environmental impacts, Sci. Total Environ. (2014) 470–471, https://doi.org/10.1016/j.scitotenv.2013.10.029.
[13] R.L. Lozano, et al., Radioactive impact of Fukushima accident on the Iberian Peninsula: evolution and plume previous pathway, Environ. Int. 37 (7) (2011) 1259–1264, https://doi.org/10.1016/J.ENVINT.2011.06.001.

[14] G. Katata, M. Chino, T. K, Detailed source term estimation of the atmospheric release for the Fukushima Daiichi Nuclear Power Station accident by coupling simulations of an atmospheric, Atmos. Chem. Phys. 15 (2015) 1029–1070, https://doi.org/10.5194/acp-15-1029-2015.
[15] A. Al-Khawlany, A. Khan, J. Pathan, Review on studies in natural background radiation, Radiat. Protect. Environ. 41 (4) (2018), https://doi.org/10.4103/rpe.rpe_55_18.
[16] R. García-Tenorio, J.P. Bolivar, M.J. Gazquez, J. Mantero, Management of by-products generated by NORM industries: towards their valorization and minimization of their environmental radiological impact, J. Radioanal. Nucl. Chem. 306 (3) (Dec. 2015) 641–648, https://doi.org/10.1007/S10967-015-4263-6.
[17] J.P. Bolívar, et al., Occupational exposures in two industrial plants devoted to the production of ammonium phosphate fertilisers, J. Radiol. Prot. 33 (1) (Mar. 2013) 199–212, https://doi.org/10.1088/0952-4746/33/1/199.
[18] C.H. Saueia, B.P. Mazzilli, D.I.T. Fávaro, Natural radioactivity in phosphate rock, phosphogypsum and phosphate fertilizers in Brazil, J. Radioanal. Nucl. Chem. 264 (2) (2005), https://doi.org/10.1007/s10967-005-0735-4.
[19] M. Charles, UNSCEAR report 2000: sources and effects of ionizing radiation. United nations scientific comittee on the effects of atomic radiation, J. Radiol. Prot. 21 (1) (2001) 83–86, https://doi.org/10.1088/0952-4746/21/1/609.
[20] K. Rosén, M. Vinichuk, Potassium fertilization and 137Cs transfer from soil to grass and barley in Sweden after the Chernobyl fallout, J. Environ. Radioact. 130 (2014), https://doi.org/10.1016/j.jenvrad.2013.12.019.
[21] G. Pucha, et al., Soil radioactivity in the highest volcanic region of Northern Andes, J. Environ. Radioact. 262 (March) (2023), https://doi.org/10.1016/j.jenvrad.2023.107142.
[22] M. Pérez, E. Chávez, M. Echeverría, R. Córdova, C. Recalde, Assessment of natural background radiation in one of the highest regions of Ecuador, Radiat. Phys. Chem. 146 (January) (2018) 73–76, https://doi.org/10.1016/j.radphyschem.2018.01.002.
[23] D. P. 2003. Hemmings, The Phosphates of Ecuador: Characterization, Genesis, and Radiological Implications. Thesis, University of Guelph, Canada, 2003.
[24] M. Kurihara, Y. Onda, H. Suzuki, Y. Iwasaki, T. Yasutaka, Spatial and temporal variation in vertical migration of dissolved 137Cs passed through the litter layer in Fukushima forests, J. Environ. Radioact. 192 (2018), https://doi.org/10.1016/j.jenvrad.2018.05.012.
[25] J.J. Kiss, E. Jong, L.W. Martz, The distribution of fallout cesium-137 in southern saskatchewan, Canada, J. Environ. Qual. 17 (3) (1988), https://doi.org/10.2134/jeq1988.00472425001700030017x.
[26] Municipio de Loja, Plan de Desarrollo y Ordenamiento Territorial Actualizado 2014- 2022, 2014 [Online], https://www.loja.gob.ec/files/image/LOTAIP/podt2014.pdf.
[27] Gobierno Autónomo Descentralizado Catamayo, "Plan de desarrollo y ordenamiento territorial de catamayo 1." [Online]. Available: https://catamayo.gob.ec/wp-content/uploads/PDOT_PUGS/PDOT-2019-2023.pdf.
[28] G. A. D. P. de Z. Chinchipe, Plan de Desarrollo y Ordenamiento Territorial de Zamora Chinchipe 2019 -2023 [Online], https://zamora-chinchipe.gob.ec/wp-content/uploads/2020/08/PDOT-2019-2023-ZAMORA-CHINCHIPE.pdf, 2019.
[29] P.G. Appleby, G.T. Piliposian, Efficiency corrections for variable sample height in well-type germanium gamma detectors, Nucl. Instrum. Methods Phys. Res. Sect. B Beam Interact. Mater. Atoms 225 (3) (2004), https://doi.org/10.1016/j.nimb.2004.05.020.
[30] M.J. Gázquez, et al., A new methodology based on TRU resin to measure U-, Th-isotopes and 210Po by alpha-particle spectrometry, Talanta 253 (September 2022) (2023), https://doi.org/10.1016/j.talanta.2022.123972.
[31] L. Hallstadius, A method for the electrodeposition of actinides, Nucl. Instrum. Methods Phys. Res. 223 (2–3) (1984) 266–267 [Online]. Available: https://www.academia.edu/30856148/A_method_for_the_electrodeposition_of_actinides. (Accessed 31 July 2023).
[32] W.W. Flynn, The determination of low levels of polonium-210 in environmental materials, Anal. Chim. Acta 43 (C) (Jan. 1968) 221–227, https://doi.org/10.1016/S0003-2670(00)89210-7.
[33] IAEA, A procedure for the determination of Po-210 in water samples by alpha spectrometry, Iaea/Aq/12 12 (2009) 42 [Online]. Available: http://www-pub.iaea.org/MTCD/publications/PDF/IAEA-AQ-12_web.pdf.
[34] P. Grinberg, S. Willie, R.E. Sturgeon, Determination of thorium and uranium in ultrapure lead by inductively coupled plasma mass spectrometry, Anal. Chem. 77 (8) (2005), https://doi.org/10.1021/ac048539t.
[35] A. Hierro, J.P. Bolivar, F. Vaca, J. Borrego, Behavior of natural radionuclides in surficial sediments from an estuary impacted by acid mine discharge and industrial effluents in Southwest Spain, J. Environ. Radioact. 110 (Aug. 2012) 13–23, https://doi.org/10.1016/J.JENVRAD.2012.01.005.
[36] M.S. Kamar, et al., An extended investigation of high-level natural radioactivity and geochemistry of neoproterozoic dokhan volcanics: a case study of wadi gebeiy, southwestern sinai, Egypt, Sustain. Times 14 (15) (2022), https://doi.org/10.3390/su14159291.
[37] UNSCEAR, Source, effects and risks of ionising radiation - exposures from natural sources of radiation, Health Phys. 647 (1988) [Online], https://www.unscear.org/docs/publications/1988/UNSCEAR_1988_Report.pdf.
[38] H.M. Abdelbary, E.A. Elsofany, Y.T. Mohamed, M.M. Abo-Aly, M.F. Attallah, Characterization and radiological impacts assessment of scale TENORM waste produced from oil and natural gas production in Egypt, Environ. Sci. Pollut. Res. 26 (30) (2019) 30836–30846, https://doi.org/10.1007/s11356-019-06183-x.
[39] J. Beretka, P.J. Mathew, Natural radioactivity of australian building materials, industrial wastes and by-products, Health Phys. 48 (1) (1985) 87–95, https://doi.org/10.1097/00004032-198501000-00007.
[40] UNSCEAR, *Sources And Effects of Ionizing Radiation*: UNSCEAR 1993 Report to the General Assembly, 1993.
[41] C.D. Mandujano-García, M. Sosa, J. Mantero, R. Costilla, G. Manjón, R. García-Tenorio, Radiological impact of natural radionuclides from soils of Salamanca, Mexico, Appl. Radiat. Isot. 117 (2016), https://doi.org/10.1016/j.apradiso.2016.01.031.
[42] S.A.M. Issa, M.A.M. Uosif, M. Tammam, R. Elsaman, A comparative study of the radiological hazard in sediments samples from drinking water purification plants supplied from different sources, J. Radiat. Res. Appl. Sci. 7 (1) (2014) 80–94, https://doi.org/10.1016/j.jrras.2013.12.006.
[43] A. Mihailović, M.V. Vasić, N. Todorović, J. Hansman, J. Vasin, M. Krmar, Potential factors affecting accumulation of unsupported 210Pb in soil, Radiat. Phys. Chem. 99 (2014) 74–78 [Online], https://www.academia.edu/10919947/Potential_factors_affecting_accumulation_of_unsupported_210Pb_in_soil. (Accessed 31 July 2023).
[44] Encyclopedia of Scientific Dating Methods, Encycl. Sci. Dating Methods (2014), https://doi.org/10.1007/978-94-007-6326-5.
[45] P.A. Ochoa, A. Fries, D. Mejía, J.I. Burneo, J.D. Ruíz-Sinoga, A. Cerdà, Effects of climate, land cover and topography on soil erosion risk in a semiarid basin of the Andes, Catena 140 (2016), https://doi.org/10.1016/j.catena.2016.01.011.
[46] K. Abad, E. Gusmán-Montalván, P. Ramón, J.I. Burneo, P. Quichimbo, L. Jiménez, Edaphic properties under Vachellia macracantha in an elevation gradient of dry scrub in southern Ecuador, J. Arid Environ. 210 (2023), https://doi.org/10.1016/j.jaridenv.2022.104878.
[47] P.S. Hameed, G.S. Pillai, R. Mathiyarasu, A study on the impact of phosphate fertilizers on the radioactivity profile of cultivated soils in Srirangam (Tamil Nadu, India), J. Radiat. Res. Appl. Sci. 7 (4) (2014) 463–471, https://doi.org/10.1016/j.jrras.2014.08.011.
[48] L. Guidotti, F. Carini, R. Rossi, M. Gatti, R.M. Cenci, G.M. Beone, Gamma-spectrometric measurement of radioactivity in agricultural soils of the Lombardia region, northern Italy, J. Environ. Radioact. 142 (2015), https://doi.org/10.1016/j.jenvrad.2015.01.010.
[49] R. badghish, S. Hamidalddin, Measurement of natural radiation, calculation of radiation doses of agricultural environmental samples in the western region - kingdom of Saudi Arabia, J. Radiat. Res. Appl. Sci. 15 (1) (2022), https://doi.org/10.1016/j.jrras.2022.01.006.
[50] R. Washington, et al., Activity concentration and mapping of radionuclides in Espírito Santo State soils , Brazil, Radiat. Phys. Chem. 167 (December 2018) (2020) 108209, https://doi.org/10.1016/j.radphyschem.2019.03.013.
[51] S.B. Ibikunle, A.M. Arogunjo, O.S. Ajayi, Characterization of radiation dose and soil-to-plant transfer factor of natural radionuclides in some cities from south-western Nigeria and its effect on man, Sci. African 3 (2019) e00062, https://doi.org/10.1016/j.sciaf.2019.e00062.
[52] N. Yildiz, B. Oto, S. Turhan, F.A. Uğur, E. Gören, Radionuclide determination and radioactivity evaluation of surface soil samples collected along the Erçek Lake basin in eastern Anatolia, Turkey, J. Geochem. Explor. 146 (2014), https://doi.org/10.1016/j.gexplo.2014.07.013.